JPIChE 53(1) 2025: 11-29

Journal of the Pakistan Institute of Chemical Engineers

Journal homepage: www.piche.org.pk/journals

DOI: https://doi.org/10.54693/piche.05312

Check for updates

Fabrication of Anion Exchange Membrane (AEM) using Polyvinylidene Fluoride (PVDF) to Separate Glycine Via Electrodialysis

M. Ahmad[1*], H.A. Mannan[1], A. Ghaffar[2], S.M. Khan[1]

Submitted: 05/03/2025, Accepted: 14/05/2025, Published: 24/05/2025

Abstract

Enormous industrial waste is produced while manufacturing food supplements, beverages, desserts, medicaments, energy drinks, tonics, and bakery items containing varying quantities of foodstuffs such as organic acids, vitamins, and amino acids derived from feedstocks. This waste is discharged into water, or is discarded in open spaces where it accumulates, contributing to environmental burden and causing millions in revenue loss annually. These crucial food items must be recovered by separating them from waste to ameliorate the economy and quality of life regarding environmental cleanliness. Anion exchange membrane-based electrodialysis has emerged as one of the most effective techniques to address these unavoidable process gaps and flaws. Polyvinylidene fluoride-based ion exchange membranes were synthesized by introducing varying amounts of ion exchange resin, applying the solution blending technique with N-Methyl 2-pyrrolidone as its compatible organic solvent, and a single-step phase inversion was opted for pore formation in deionized water-ethanol solution. Subsequently, each membrane was modified with polyaniline coating to enhance its conductivity, ion exchange capacity, superhydrophilicity, and anion exchange capability. The effect of polyaniline coating and varying quantities of ion exchange resin incorporated while fabricating membranes in Polyvinylidene fluoride matrix was studied in terms of its separation efficiency of glycine via electrodialysis in feed and glycine product solutions as glycinate ions quantifying with acid-based titration which found to be enhanced from 10% to 43% and verified with HPLCMSMS. These membranes can be considered as a novel approach for developing an efficient, modern anion-exchange membrane system on an industrial scale for commercial applications.

Keywords: PVDF, Ion Exchange Resin, PANI, IEMs, Electrodialysis, HPLC.MSMS

1. Introduction:

Membrane technologies such as membrane distillation, reverse osmosis, microfiltration, nanofiltration, and ultrafiltration are extensively used in food, petrochemicals, pharmaceuticals, and many other industries [1-4]. One of the widely used membrane fabrication materials designated for ultrafiltration and microfiltration is polyvinylidene fluoride (PVDF), which is a mechanically and thermally stable thermoplastic polymer, maintaining marvelous resistance to ultraviolet radiation and corrosive chemicals with superior electro-active properties. Among all the fluoroplastics, it ranks in second position due to its utility in terms of production volume [3-7]. Electrodialysis is one of the unique techniques involving an ion exchange membrane (IEM) for concentrating, purifying, and separating ionic solutions [8-10]. The IEM is a charged membrane extensively used in electrolysis, electrodialysis, and diffusion dialysis. It functions as an ion-selective barrier and an excellent key to separation techniques [11]. Selectivity and conductivity are the two unique features

[1]*Institute of Polymer & Textile Engineering, University of the Punjab, Lahore 54590, Pakistan*
[2]*Department of Chemistry, University of Engineering and Technology, Lahore 54890, Pakistan*
*** Corresponding author:** Munir Ahmad (munirahmad.IPTE@gmail.com)

of an IEM, but it is impossible to attain their optimum values simultaneously [12]. The most recent economic developments forecast that membrane technology may be considered the latest technology regarding the purification and separation of materials at the micro-level. Different techniques have been applied for synthesizing IEMs, including solution blending, grafting, plasma, electrochemical, and *in-situ* polymerization [13-17]. A new era of membrane surfaced when IEMs were synthesized by blending cation and anion exchange resin with polymer in its compatible solvent by following the solution blending technique, and the surface of such membranes was modified by coating with some intrinsically conducting polymer (ICP) to widen its role and application areas [18]. The development and surface modification of IEMs was carried out by dip coating, *in situ* polymerization, atom transfer radical polymerization, electrochemical growth, spin coating, grafting, thermally induced grafting, and immobilization [16-22]. Spin coating is simple and produces a smooth, ultrathin polyaniline (PANI) film on the membrane surface. Polyaniline is a low cost, stable, easily available ICP, and with simple and easily tunable chemistry by treating it with some acid or a base, but its insolubility in most solvents restricts its extensive use as a modifying agent [23]. Membrane morphology and its performance depend on selecting a compatible solvent with the ion exchange resin and polymer [24]. Among many ICPs, PANI is one of the most extensively researched ICP with a lot of versatile applications in almost every industry like food, pharmaceutical, beverage, ink, dyes, solvent extraction, chemical and petrochemical industries in terms of separation requirements on account of the molecular size of the solution [9, 25-27]. PANI got immense attention for its use as a surface modifying agent of the IEM, whereas the incorporated IER functions as the performance additive in separation activities in addition to its mechanical support [28]. The PANI film's morphological and electronic characteristics depend upon the substrate surface's nature regarding its hydrophobicity or hydrophilicity [29]. Sapurina determined that when aniline oligomers are adsorbed on the rough surface of the substrate, they develop smooth and groove-free PANI film [30]. Superior conductivity and mechanical properties can be acquired simultaneously for a desired purpose by judicious choice of molecular weight of the base polymer and processing conditions [31]. The chemical and bio-chemical industries opted for IEMs of different sizes and thicknesses fabricated using various polymeric materials that are intelligently intriguing and have performance additives for their separation needs, which are advanced separation tools. IEMs are being applied in pervaporation, electrodialysis, nanofiltration, ultrafiltration, and to separate gases [32-37]. Glycine is an amino acid that is a vital ingredient for the human body, existing in anionic, neutral, or cationic forms depending upon the pH of the liquid [38, 39]. The transport mechanism of glycine is based on interfacial chemical reactions due to the exchange of ions, like in Donnan dialysis, but the transfer rate of ions depends upon the nature of the anion exchange membrane (AEM) and the number of ionic species present in the feed solution [40, 41]. Electrodialysis has gained immense focus on production, separation, purification, and concentrating food acids like ascorbic acid, lactic acid, tartaric acid, and amino acids, from the feedstock, reaction broths, and wastewater due to their deterioration causing an unfriendly environment and promoting ill effects on the ecosystem [42, 43].

The prime focus of this instant research work is to develop a PANI-modified AEM prepared by mixing mecolite PA101 in PVDF matrix through solution blending for the separation of glycine via electrodialysis which is an important ingredient of food supplements, beverages and has potential applications in pharmaceutical industries and its scarcity may lead to some ill effects on the economy in terms of its urgent import by incurring precious foreign exchange [3, 4, 44, 45].

2. Experimental:

2.1 Materials:

Mecolite (PC003ID/PA101) is a cation and anion exchange resin consisting of Polystyrene-divinylbenzene-trimethyl ammonium chloride (PS-DVB-TAC) and sulfonated polystyrene divinylbenzene (SPS-DVB), respectively, which were taken from a local market and applied after micronizing them up to 400 mesh. A Lahore-based plastic company provided the polyvinylidene fluoride. The polyaniline, ferric chloride ($FeCl_3$), phenolphthalein, hydrochloric acid, sodium hydroxide (NaOH), and analytical grade glycine were obtained from Merck and Sigma-Adrich, respectively. The PVDF, glycine, reagents, and various other chemicals were pure, moisture-free, and of analytical grade, and were applied without further purification or

pretreatment. The entire experimental work was carried out using deionized water.

2.2. Synthesis of Polyvinylidene Fluoride (PVDF) Membrane:

2.2.1. Fabrication of 15%PVDF-based ion exchange membranes (IEMs):

Initially , S–DVB–TAC and SPS–DVB were soaked in water for 24 hours and pulverized in a rod mill. Each resin was micronized and used after sieving through a 400 mesh. Later, PVDF was micronized using a pestle and mortar and allowed to pass through a 400-mesh. Prepared the 15%PVDF-based 100:0, 90:10, 80:20, 70:30, 60:40, and 50:50 cation and anion exchange casting solution by mixing 0-0g, 0.19g, 0.5g, 0.89g,1.41g, and 2.15g of cation and anion exchange resin in addition to 2.25g of PVDF in each solution separately, being a constant quantity, and made the volume of every concentration 15 mL by adding N-methyl-2-pyrrolidone [46-49]. Warmed each solution at 60°C to develop a homogeneous, clear, free-of-bubbles casting solution, and all the solutions were placed in an air-tight, moisture-free, non-corrosive glass container in a dark place for 48 hours so that each solution could be ready for casting into the membrane. The composition and synthesizing scheme of every solution is given in the Table.1

Table 1: Synthesis of 15%PVDF-based cation and anion exchange casting solution and water uptake of the synthesized membranes

S.No	NMP (mL)	PVDF (g)	Anion/Cation Exchange Resin	Concentrations (PVDF: IER)	Casting solution	**Water uptake Percentage after**		
						2h	8h	12h
1	12.8	2.25	0.00g	Blank	Pure PVDF-casting solution	0.01	0.02	0.034
2	12.56	2.25	0.19g	90:10	15%PVDF-based cation\anion exchange casting solution	7.18	14.98	16.09
3	12.25	2.25	0.5g	80:20	15%PVDF-based cation\anion exchange casting solution	18.54	28.32	30.09
4	11.86	2.25	0.89g	70:30	15%PVDF-based cation\anion exchange casting solution	20.64	29.832	33.098
5	11.34	2.25	1.41g	60:40	15%PVDF-based cation\anion exchange casting solution	23.06	28.871	36.098
6	10.6	2.25	2.15g	50:50	15%PVDF-based cation\anion exchange casting solution	27.09	34.09	39.08

Later, numerous 100µm thick non-composite and composite anion and cation exchange membranes were synthesized using this casting solutions that were cast into cation and anion exchange membranes on a groove-free, plain and ultra-smooth glass plate by using a casting knife [50, 51]. All the membranes were kept in the open air for 3 h at 25 ˚C so that the solvent could be evaporated and transferred into a deionized water-ethanol bath for 48 hours so that single-step phase inversion may occur. Each membrane was hydrolyzed in 1 M NaOH solution for 1 hour, then washed separately with deionized water and preserved after drying for further use.

2.3. PANI-Coating on Non-composite and Composite Ion Exchange Membrane

Prepared 0.4M aniline chloride and 0.3M $FeCl_3$ solutions by dissolving 3.7 mL of aniline and 4.8g of $FeCl_3$ in 96.3 and 95.2 mL of 0.4M HCl solution. Both solutions were mixed until a grassy green color was developed. The membranes already fabricated by using casting solutions based on varying quantities of (PS-DVB-TAC)/(SPS-DVB) in a fixed PVDF quantity were dipped into the grassy green polyaniline solution for its *in situ* polymerization for 24 h [52]. Subsequently, each PANI polymerized membrane was neutralized with 0.1 M HCl so that oligomers of PANI could be washed away if any were present at the membrane and again rinsed with deionized water. Dried each membrane in an oven at 50 ˚C for 24 h, and preserved in an air-free box for further use. The expected mechanism of the PANI-coating on the membrane is described in Figures 1 & 2 below, indicating a reaction among the ion exchange resin, PVDF, and PANI when they encounter.

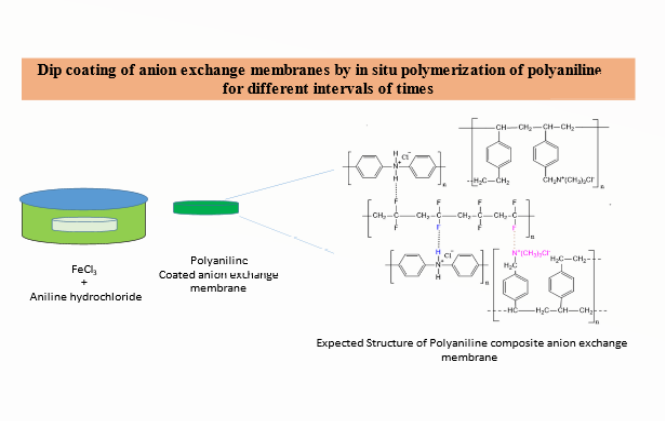

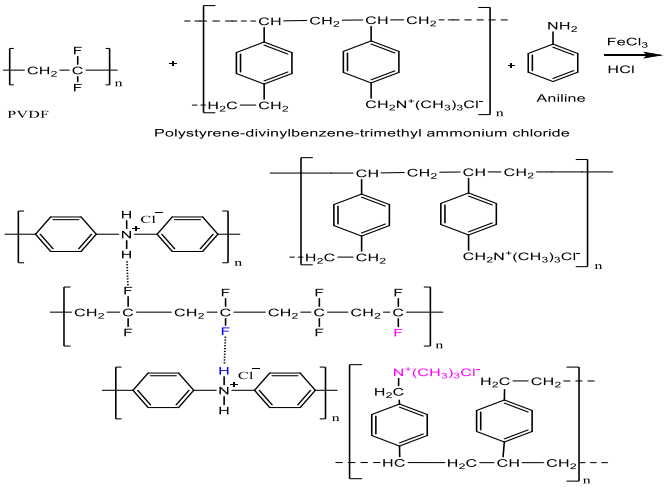

Figures 1&2: Expected route and reaction mechanism of PANI-coating by *in situ* polymerization on the surface of 15%PVDF-based composite membranes [53, 54]

3. Properties and Characterization of IEM:

3.1. Water Uptake:

A 2 cm^2 piece of the membrane was dipped in deionized water for 24 h to attain equilibration, and the closed voids may also open. The membrane swelled up, and its weight increased due to water uptake [55-57]. The membrane was weighed after squeezing out its excessive water with tissue paper and dried in a temperature-controlled oven for 4 hours at 70 °C, and it was weighed again. The difference in mass between wet (W_{wet}) and dry (W_{dry}) was calculated, which led to determining water uptake percentage (%) measurement by the following formula [58-60].

$$\mathbf{Wateruptake}(\%\mathbf{age}) = \frac{\mathbf{W_{wet} - W_{dry}}}{\mathbf{W_{dry}}} \times \mathbf{100} \quad (1)$$

3.2. On Exchange Capacity(IEC) of Ion Exchange Membranes:

30 mL of 0.1 M NaOH solution was prepared, and a 2 cm^2 piece of PANI-coated AEM was kept in it for 24 hours. The chloride ions (Cl^-) were replaced by the hydroxyl (OH^-) ions, which are the quinoid part of the PANI-coating of the AEM, and of the quaternary ammonium, which is of the anion exchange resin, respectively [61-63]. The depleted hydroxyl ions (OH^-) are ascertained by titrating with 0.1 M HCL. Weigh the samples after washing and drying. The IEC was ascertained as meq/g of the depleted hydroxyl ions (OH^-) per gram of dry IEM Eq-2. [59].Table 2

$$\mathbf{IEC(meq/g)} = \frac{[V_{NaOH}(N_1 - N_2)]}{W_{dry}} \quad (2)$$

Table 2: IEC and conductivity of the non-composite and composite-AEMs synthesized using 15% PVDF mixed with 10%, 20%, 30%, and 40% mecolite PA101

S.No	Membrane composition and its category	IEC (meq/g)	Conductivity (Scm^{-1})
1	100µm thick, uncoated pure PVDF membrane	0.890	$0.211x10^{-8}$
2	100µm thick, PANI-coated, PVDF membrane	1.198	$0.880x10^{-7}$
3	100µm thick,PANI-coated, PVDF+mecolite PA101(90:10) membrane	1.201	$0.890x10^{-7}$
4	100µm thick, PANI-coated, PVDF+mecolite PA101(80:20) membrane	1.239	$0.921x10^{-7}$
5	100µm thick, PANI-coated, PVDF+mecolite .PA101(70:30) membrane	1.248	$0.942x10^{-7}$
6	100µm thick, PANI-coated, PVDF+mecolite PA101(60:40) membrane	1.257	$0.960x10^{-7}$

3.3. Electrical Conductivity:

The four-probe method was applied to determine the electrical conductivity of a 3 cm^2 spherical piece of IEM with the help of Keithley, 6220-Precision being a source of current, while the potential difference is applied by PS3030-DD. The space between the probes is 0.2 cm which is due to their negligible thickness ranging from 130–40 µm when their thickness is compared with the space between each probe while Equation (3) ascertains its value and is found to be in the range of 0.20×10^{-8} to 0.92×10^{-8} (Table 2) [64].

$$\mathbf{Resistivity}(\boldsymbol{\rho}) = V_{IC}\left(\frac{d}{s}\right) \quad (3)$$

V, *I, and C* are voltage, current, and correction factors. The value of *C* is obtained when the membrane diameter (*d*) is divided by space (s), while the membrane conductivity is ascertained by taking the inverse of the resistivity [65].

$$\mathbf{Conductivity}(\boldsymbol{\sigma}) = \mathbf{1/Resistivity} \quad (4)$$

3.4. Structure Elucidation by FTIR Spectroscopy:

The functionalities of each IEM were ascertained by applying the JASCO FTIR-4100 (developed in Tokyo, 193-0835, Japan) equipped with ATR in the range of 4000-600 cm^{-1}.

3.5. Thermogravimetric Analysis (TGA):

The TGA of each IEM was determined using SDT-Q600 developed in New Castle, DE 1972, USA at 20°C/min heating rate in an inert atmosphere of constantly flowing nitrogen gas.

3.6. Scanning Electron Microscope (SEM) Analysis:

FEI INSPECT 550, a scanning electron microscope developed in São Carlos, SP-BR, CEP 13565-906, Brazil, was applied to record the surface morphology of every membrane at various resolutions.

3.7. Particle Size Distribution Analysis:

The shape and size of micronized resin and PVDF particles were determined by applying the Litesizer-500 developed in Anton Paar-GmbH, Germany, in order of 1.976–2.964 µm tiny granules (Figure 3), and its effect on membrane morphology was examined by SEM analysis.

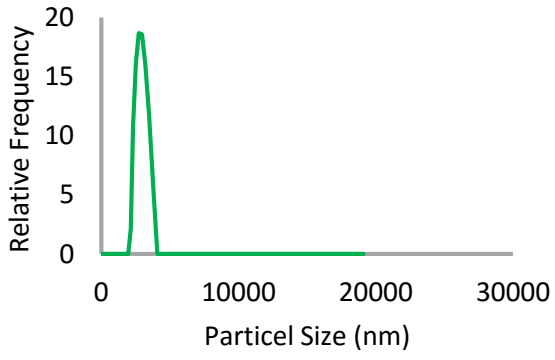

Figure 3: Analysis of particle size of PVDF, anion, and cation exchange resin using a size analyzer

3.8. Membrane Thickness:

The thickness of each dry membrane was determined by a digital thickness gauge meter developed by Mitutoyo, Schenectady, NY, USA.

3.9. Electrodialysis:

Electrodialysis was conducted in an electrodialyzer made of glass with four compartments. The cathode and anode are composed of titanium and steel plates, whereas the open area of each electrode is 12.56 cm^2. The AEM, acting as a test membrane, was fixed in the middle while the CEMs of identical composition and thickness to that of the AEM were placed on either side in the electrodialyzer. The chambers adjacent to the cathodic and anodic compartments were tagged as feed and product chambers, and both were filled with 7.5 mL of 1% glycine solution, and same quantity equal to glycine of 0.5M NaOH solution was loaded as an electrolyte in the anodic and cathodic compartments. Every AEM was kept in glycine solutions for 48 hours before the electrodialysis to ensure its acquaintance with the glycine solution.

1. Glycinate ion (Feed Chamber)____**AEM**___ Glycinate ion (Product Chamber)
2. Sodium ion (Anodic Chamber)____**CEM**____ Sodium ion (Product Chamber)
3. Sodium ion (Feed Chamber)____**CEM**___ Sodium ion (Cathodic chamber)

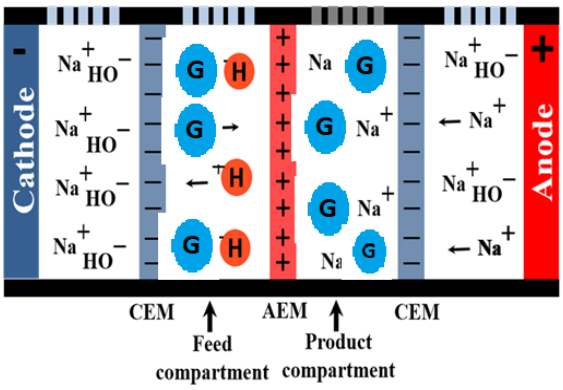

Figure 4: Electrodialysis of glycine [66-68]

Table 3: Electrodialysis of 1%aqueous glycine solution using pure, uncoated, and polyaniline-coated 15%PVDF-based composite and non-composite membranes and their efficeinvy by LCMS and titration method

S.No	Membrane category and its composition	Voltage	Current in 30 min	%Efficiency by	
				LC MS	Titration
1	100µm thick, pure PVDF membrane	31.4	0.23	4.21%	4.650 %
2	100µmthick,PANI-coated PVDF membrane.	31.4	0.28		
3	100µmthick,PANI-coated,PVDF+mecolite-PA101(90:10)membrane.	31.4	0.70	9.81%	9.756 %
4	100µmthick,PANI-coated,PVDF+mecolite-PA101(80:20)membrane	31.4	0.09		
5	100µmthick,PANI-coated,PVDF+mecolite-PA101(70;30) membrane	31.4	0.08	9.81%	9.756 %
6	100µmthick,PANI-coated,PVDF+mecolite-PA101(60:40)membrane.	31.4	0.69		

The anode and cathode terminals were attached to a direct current after being loaded with feed, electrolyte, and product solutions in respective chambers. Once the potential difference was applied, the ions began to migrate through the IEMs, resulting in vigorous bubbling with an instant rise in temperature, indicating that electrodialysis had begun, leading to a surge and decline in the volume of the product and feed solutions, respectively. The glycinate ions resulting from the electrodialysis of glycine in the feed chamber started to migrate into the product chamber after passing through the AEM by decreasing and increasing the volume of feed and product solutions. The sodium ions entered the cathodic chamber after passing through CEM from the feed chamber. The anodic chamber is the hub of sodium ions (Na^+) ions and they migrate to the product chamber to balance the negatively charged glycinate ions ($^-$Ve). This setup promotes the movement of ions in the electrodialyzer under the influence of direct current, which is a driving force. The variation in current was observed while a 31.4 V remained constant, during the 30-minute electrodialysis. (Table 3). The efficiency of AEM was quantified by titrating separated feed and

product solutions before and after electrodialysis with HCL, and HPLC verified its results [68, 69].

3.10. Quantification of Electrodialysis Result:

The electrodialysis result was quantified by the titration method and verified using HPLCMSMS. The performance of AEMs was monitored by titrating product and glycine feed solutions separated as a result of electrodialysis using AEM with HCL using phenolphthalein as an indicator [68].

Glycine is separated into feed and glycine product solutions containing varying numbers of glycinate ions on electrodialysis using pure and PANI-coated AEM made of PVDF. The result was quantified by HPLCMSMS, confirming the efficiency of AEM regarding glycine separation. Four working standards of 100, 250, 500, and 1000 ppb concentrations were injected into the HPLC.MSMS. Then the samples were allowed to be sucked by LC after diluting them through the autosampler and subsequently shifted into the mobile phase which carries it into the column. The triple quad is a sensitive component. and its column acts as the stationary phase, and separates the glycine from the mixture, The glycine enters the triple quad of MS if the sample contains it and is ionized here by electron spray (ESI), generating 73 precursor ions. These precursor ions plunge into the quadrupole, where they are identified and moved into the inert atmosphere of the collision cell created by the nitrogen gas. MSMS is applied to detect and quantify precursor ions. The precursor ions further disintegrate into 30.1 product ions, which appear on the calibration curve. This ion is identified after the second quadrupole. The calibration curve based on 4 points was drawn with linearity R^2=0.996, and the glycine peak was identified at 13.57 minutes retention time. The last column in the quantitative summary report is the final concentration in parts per billion. The result of each sample was ascertained by comparing the peak of the standard sample by applying the Mass-Hunter software for quantitative analysis. The number of separated glycinate ions increases as the electrodialysis of 1% glycine advances, increasing the peak area in the chromatogram that is calculated considering the retention time. The AEM efficiency is evaluated in terms of the final concentration of glycine in the form of separated glycinate ions and its quantification by LC-MS/MS in each sample, applying the following formula

Percentage (%) of Glycine =Concentration from calibration curve x Total volume x dilution factor/Weight of the sample

4. Results and Discussion:

4.1. Water uptake:

The pure PVDF membrane is hydrophobic as it absorbed 0.4% of water in 24 h, which cannot be considered an appreciable water uptake [70]. Water uptake values of plain and PANI-coated AEMs are given in Table 1**,** which shows an increasing trend with a gradual increase in resin quantity. The water uptake has increased from 0.04% to 46%. It might have resulted from incorporating more hydrophilic bulky functional groups and other charged moieties into the membrane phase, such as quaternary ammonium chloride and divinylbenzene (DVB) in specific volume, which became hydrated by the electrolyte in water and responded with more swelling of the membrane [71]. The water uptake by PANI-coated, resin-incorporated AEM is exorbitantly higher than that of the PVDF and PANI-coated PVDF membranes, which is totally due to the structural interaction of (PVDF+PS-DVB-TAC) PANI with the water. The PS-DVB-TAC/10%, 20%, 30%, and 40% PANI-coated PVDF membranes absorbed 34%, 36%, 39%, and 45% water respectively, and this convincing increase was assigned to the high contents of DVB, quaternary ammonium, chloride ions and method of fabrication in addition to hydrophilic moieties in polyaniline [72]. The PVDF/PS-DVB-TAC blending inculcated the hydrophilic properties in the PVDF, which facilitated the water plasticization effects and resulted in more interaction between PVDF and water, causing a highly membrane-swollen morphology [73]. The enhanced Hydrophilic character, which is developed due to the introduction of ion exchange resin in the PVDF, promoted the physical cross-linking between water-PANI and water-ion exchange resin in addition to water-polymer, polymer-polymer, which is capable of forming a polymer gel-like structure while absorbing water in the regions that were developed due to cross-linking, whereas such a structure is thermally reversible. The structures, which promote gel-formation, permit the excessive moisture to be absorbed while residing in the polymer phase, promoting water absorption in IEM [74, 75]. This enormous swelling may also be linked with some unique morphology of PANI-coated resin-

incorporated IEMs, which resulted from robust H-bonding between water-PANI and resin-PANI in addition to PVDF-resin and PVDF-PANI moieties in the backbone of the chains. This robust hydrogen bonding promoted relatively more swelling that enhanced water uptake quite significantly in IEMs when compared to other IEMs of similar structure [66]. The water uptake by the IEMs is also associated with the concentration of doping acid, which increased on increasing the concentration of the doping acid in PANI increased, which was consumed during its preparation. This reasonable increase in water uptake is rightly attributed to the synergetic effects of quaternary ammonium chloride (QAC), Divinvylbenzene (DVB), quinoid, and the bulky benzenoid moieties in PS-DVB-TAC and in PANI with enhanced duration of absorption which fully supports to fill the voids, gaps, and free volume in the molecules of the membrane as such increasing the membrane swelling ratio manifold by increasing water absorption capability of the membrane [76] as presented in Table 1.

4.2. Particle Size Analysis:

The mecolite (PA101/PC003ID) was micronized in the range of 1.976–2.964 μm and this is close to 2.3–2.6 μm as that particle size is extensively used in the synthesis of membrane exhibiting a smooth surface by the uniform dispersion of the particles in the membrane matrix, as shown in Figure 3. The division of particles according to size is vital because it influences the phase morphology and topography of the membrane surface [77, 78]. The finer size of ion exchange resin particles may promote a uniform, smooth, and groove-free homogenous phase morphology of the membrane, and if resin grains are coarser, the phase morphology will be disturbed, and these coarser particles may impart a rough surface to the membrane. PVDF is a film-forming polymer, whereas the resin particles are relatively infusible and are unable to produce a thin film; hence, if the size and shape of tiny resin grains become coarser and irregular, it will affect the continuous film development and mechanical stability of the membrane, which is evident from SEM images.

4.3. Ion Exchange Capacity (IEC):

The IEC is a key and unique feature of a transport membrane to develop its transport characteristics more profoundly according to the specific areas of its application. The values of the IECs vary from 0.89 to 1.257 on account of pure, PANI-coated, and PANI-coated PVDF-based composite membranes fabricated by mixing 10%, 20%, 30%, and 40% anion exchange resin in the matrix of PVDF (Table 2). It is evident from the increasing trend of IEC that PANI-coating and the gradual increase in resin have a marked effect on enhancing the IEC of the membranes. The values of IECs of PANI-coated IEMs which have resin quantity in the range of 10%, 20%, 30%, and 40% by weight and dense PANI-coating increased from 1.201 to 1.257 because of the synergic effect of exchangeable chloride ions (Cl^-) with hydroxyl ions (OH^-) caused by leaching of chloride ions when the IEMs were kept in NaOH solution. It is evident from Table 2, that the IEC of PANI-coated AEM having resin and polymer quantity in the ratio of 10% and 90% respectively is 1.201 and it is enhanced up to 1.257 when the resin quantity enhanced gradually up to 40% by weight while decreasing the weight of polymer with the same ratio. It is being observed that, as the resin quantity is increased gradually from 10% to 40% by weight and PANI-coating by in situ polymerizing IEMs, the efficiency of the membranes is also enhanced from 13% to 43% in terms of separating glycine with an increase in IEC which is from 1.201 to 1.257 as such the membrane efficiency is linked with ion exchange capacity of the membranes [67].

4.4. Electrical Conductivity:

The ability of an IEM to transfer current is the conductivity of an IEM, which depends on the IEC and the charge that is fixed on it. The conductivity follows the nature and type of the counter-ions with the equilibrium concentration of the ionic liquid, while it decreases as the size of the participating ions increases [79-82]. The conductivity of the uncoated, pure PVDF membrane was $0.21x10^{-8}Scm^{-,1,}$ and it enhanced up to $0.96x10^{-7}Scm^{-1}$ when the PVDF was substituted with 10% to 40% of anion exchange resin by weight, and the surface of each membrane was modified by PANI-coating [83, 84]. The conductivity of the IEMs was enhanced in the order of $0.89\times10^{-7}Scm^{-1}$ to $0.96\times10^{-7}Scm^{-1,}$ which is attributed to the incorporated resin that has enhanced the number of exchangeable chloride (Cl^-) ions. The enhanced chloride ions from 10% to 40% in the form of ion exchange resin and PANI-coating are responsible for exchanging more glycinate ions, enhancing the glycine separation from 13% to

43%, and verifying the performance efficiency of the AEM and indirectly linking it with conductivity (Table 2).

4.5. FTIR Analysis of PANI-coated 15%PVDF-based Membranes:

The FTIR technique was applied to identify functionalities in PANI-modified IEMs prepared using PVDF as a base polymer (Table 4, Fig.6 &7). A small but flat and sharp peak is visible around 763 cm−1, depicting α-phase, while its small size indicates its poor concentration in the PVDF structure [85]. A significant and of considerable sized peak is noticed at 840 cm−1, representing the β-phase quite similar to two other peaks one around 1431 cm−1 and the other at 1276 cm−1, establishing the crystalline phase in PVDF while the peak at 1074 cm−1 is also assigned to the β-phase, which specifically exists in the structure of PVDF [86-89]. Compared to the Fluoride family, another sharp peak is noticed at wave number 794 cm−1 due to the rocking vibration assigned to -CH_2- establishing a close link to α-phase and the β-phase in PVDF while the band positioning at 2974 cm−1 is specifically designated to -CH_2- symmetric stretching, associated with β-phase and such bands are the exclusive property of PVDF polymer [90-92].

Table 4: Some Infra Red peaks in Polyaniline modified, Non-composite, and composite-IEMs, synthesized using PVDF as a base polymer mixed with mecolite (PA101/PC003ID)

S.No.	Wave Number (cm^{-1})	Assigned to
1	441,500,600,751 Rocking and Bending	CF_2,β-phase
2	834-Asymmetrical stretching	CF_2 β-phase
3	493-Bending and waging	CF_2,α-phase
4	872-Asymmetrical stretching	-C-C-C-
5	2930-Stretching	C–H
6	3372-Stretching	N–H PANI
7	1505-Stretching	C=C-[quinoid-ring]
8	1398-Stretching	C=C-[benzoid-ring]
9	2974-Symmetric stretching	-CH_2-

On comparing the positions of phase peaks, the peak regarding α-phase is more conspicuous, prominent, and pronounced in pure PVDF than in PVDF incorporated with mecolite (PC101/PC003ID), indicating that the ratio of α-phase and β-phase is significantly changed and favors β-phase instead of pure PVDF[93]. It would mean that when mecolite (PC101/PC003ID) is blended into the PVDF matrix, the PVDF will be more inclined toward the β-phase with substantial increases in its concentration. There is a characteristic and prominent peak among so many other peaks that can be noticed around 1233 cm−1, which exclusively stands for the γ-phase [51, 94] whereas, the peak at 1187 cm−1 is attributed to the combined effect of β and γ phases.

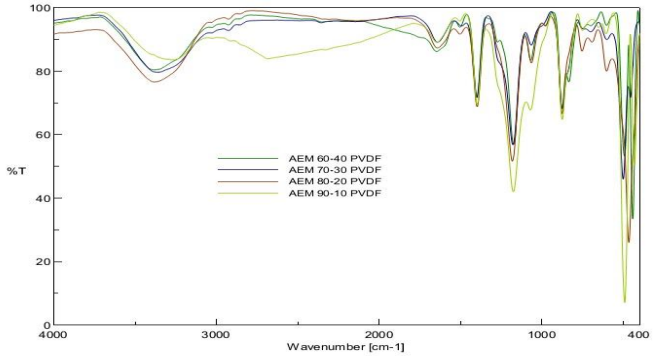

Figure 1: FTIR analysis of PANI-modified non-composite and composite AEMs synthesized by 100%, 90%, 80%. 70%, and 60% PVDF mixed with 0%, 10%, 20%, 30%, and 40% mecolite PA101 respectively

There are two other peaks, one at 885 cm−1 and the other at 1401 cm−1, indicating the combined impact of α, β, and γ phases [51, 94] while the peak around 834 cm^{-1} verifies the CF_2 in PVDF.[95].The asymmetric stretch is assigned to the β phase in PVDF which is also verified by the well-defined peaks at 441cm^{-1}, 500cm^{-1}, 600cm^{-1}, and 751 cm^{-1} mainly stands for the bending and some rocking motions of CF_2. in PVDF molecule and two other transition bands are also visible in the PVDF chain at 1170 cm^{-1} and 1231cm^{-1} directly relating to C–F stretch [96]. A well-pronounced, broad, and sharp band is identified in the middle of 3300 cm−1 &3500 cm−1, corresponding to the stretching vibration of the -OH group of bound water in the polymeric matrix [97]. The peak at 493 cm^{-1} represents the bending, wagging vibration of CF_2, showing the presence of α-phase in PVDF polymer. The peak at 872 cm^{-1} represents the asymmetric stretch due to the –C-C-C- bond in the polymeric chain of the PVDF molecule, and the peak

around 865 cm^{-1} represents the quaternary ammonium (CN^{+}) functionality in the anion exchange resin.

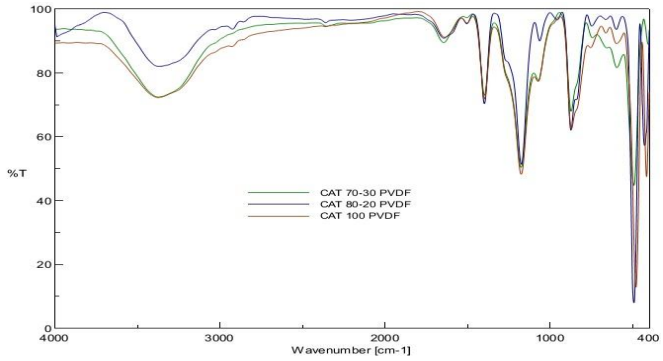

Figure 2: FTIR analysis of PANI-modified, non-composite and composite-CEM synthesized using 100% 90%, 80%, 70%, and 60% PVDF mixed with 0%,10%, 20%, 30%, and 40% cation exchange resin (mecolite PC003ID) respectively

Some characteristic and important bands appearing at wave numbers 1398 cm^{-1} and 1505 cm^{-1}well correspond to -C=C- stretching vibration present in benzenoid and quinoid rings, and the peak that appeared at 3370 cm^{-1} is due to N–H moiety in PANI molecule. The widening of this peak represents H-bonding between the C-F group of PVDF and N–H of polyaniline. There are a few other characteristic bands that might be related to PANI, such as N–H stretch at 3430 cm^{-1}, aromatic C–H stretch at 2920 cm^{-1},1494 cm^{-1} stretch of the benzene ring, and a very conspicuous and prominent peak around 1585 cm^{-1} corresponds to the stretching frequency of the quinoid ring [54, 98, 99] confirming the PANI deposition on the membrane surface [100].

4.6. TGA of PANI-coated,PVDF-based, Pure and Composite Ion Exchange Membranes:

TGA provides some practical, crucial, and functional information about the thermal stability of a membrane [101]. Mainly two and three degradation zones are prominent in the TGA profile of PANI-modified, non-composite, and composite-AEMs. The PVDF degradation starts around 400°C but when it is coated with PANI then substantial weight loss occurs at low temperatures due to weak intermolecular forces caused by PANI-coating [102, 103] (Fig.8). The thermogram of PVDF shows weight loss around 150°C or at relatively high temperature, which may be in the range of 150°C directly associated with the loss of trapped water. The removal of dopants, bound water, residual solvents, and HCL deposited when PANI was doped by in situ polymerization at the membrane surface at this temperature did not occur appreciably, and resultantly, no substantial decrease in the weight was noticed between 100 °C and 425 °C, but it took place above 425°C, and it is rightly assigned to the degradation of the polymeric chain[104-106]. The TGA is indicative that the blend in the compositions has some stability that is close to the stability of the pure PVDF molecule. The ionic salvation enhances water absorption for the doped polyaniline [107]. The major and maximum weight loss occurs at the second degradation zone, starting from 425 °C to 600 °C, when the PVDF structure fully deteriorates, and the maximum weight loss is observed at 475°C [108]. The main end products of PVDF degradation at 600°C and above are the ash and other carbonaceous polymeric residues It is interesting that the polyaniline deposition has increased the membranes' decomposition temperature to the tune of 600°C, while the literature reports it up to 500 °C as such the PANI coating has raised the thermal stability of the PVDF membrane. Three degradation zones are prominent in polyaniline-coated composite-AEMs synthesized by introducing anion and cation exchange resin in the PVDF matrix. A minute but gradual weight loss is observed as compared to the (PVDF+PANI) membrane occurs in the temperature zone of 25^{o}C - 200^{o}C which indicates the removal of trapped moisture contents in mecolite (PA101/PC003ID) an anion and cation exchange resins respectively along with other volatile components like a residual solvent and HCl which was used while doping polyaniline.

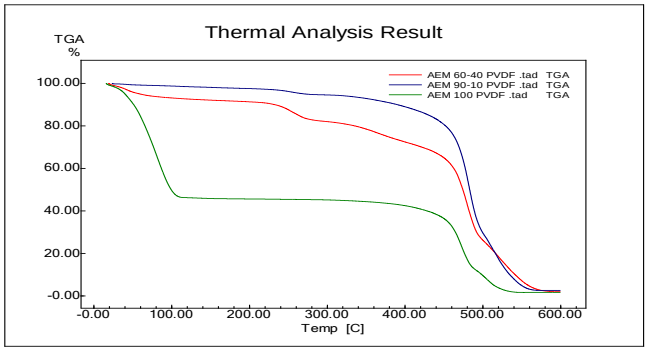

Figure 8: TGA profile of PANI-modified non-composite and composite-AEMs [105, 106, 108].

The decomposition in the second stage occurs at 200-450 °C, which is assigned to the deamination of some important parts of anion and cation exchange resins,

which is the quaternary ammonium moiety, and the decomposition of the whole anion and cation exchange resin itself. The final and third stage of weight loss falls between 400°C to 600°C which is assigned to the decomposition of the PVDF molecule itself and PANI as such it verifies that the PANI-coating enhances the thermal stability of these membranes and the incorporated mecolite (PA101/PC003ID) increases the water contents in the membrane due to the inclusion of bulky hydrophilic moieties [109]

4.7. Surface Morphology of PANI-modified, 15 % PVDF-based Membranes:

Figure 10(a) represents an SEM image of the membrane synthesized using pure PVDF, depicting a smooth but compact surface with tiny pores equipped with fibrous, delicate crystalline mass lying on the membrane surface. Figure 10.(b-e) illustrates composite membranes based on PVDF blended with anion exchange resin in the ratio of 10(b)-90:10, 10(c)80:20, 10(d)-70:30, and 10(e)-60:40 respectively, Moving from Figure 10(b) to 10(e) while examining images, it is evident that the PANI-coating is compact, with aggregation of worm-like fibrous mass embedded with minor cracks and equipped with pores of various size and diameter, haphazardly distributed having relatively rough and scaly membrane texture indicating agglomeration of some particles at the surface [110, 111]. The top surface maintains a porous structure developed by interconnected holes, which are further connected by a network constructed with small spherical particles, linked all around, forming a network. The SEM images indicate that the outer top layer of the membrane has few closed pores, showing good adherence between the permselective polymeric layer and the macroporous PVDF membrane. This phenomenon exhibits that the rapid coagulation of polymeric film deters the ultimate infiltration of separating solution into the porous PVDF membrane. The doped PANI is deposited on the membrane to enhance its hydrophilicity, improving its ion exchange capability and expanding its application areas [100]. A robust interaction has been observed between key component of PANI which may be the benzenoid (N-H) or the quinoid (–N=) with the polar parts of the anion exchange resin such as chloride (Cl^-) and the quaternary ammonium moieties in anion exchange resin, and it may have resulted in the thicker and dense coating of polyaniline..

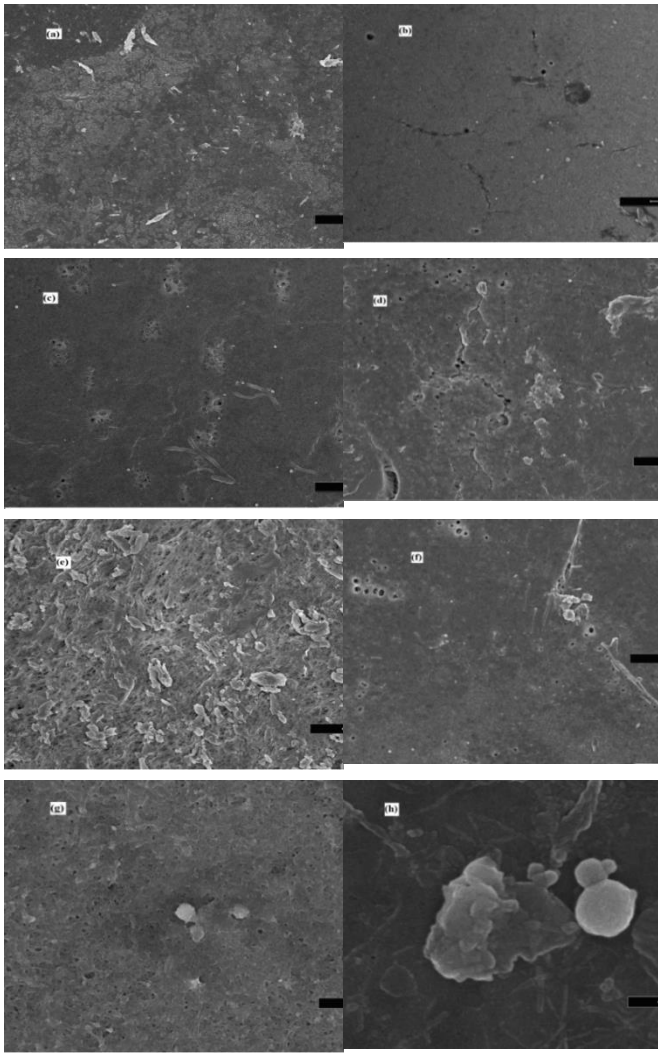

Figure 9: SEM micrographs (a) of pure PVDF membrane 10.[b-e] and 10.[f-j] PANI-coated IEMs synthesized by incorporating 10%,20%,30%, and 40% mecolite (PA101/PC003ID) anion and cation exchange resins, respectively, in the matrix of 90%, 80%,70%, and 60% PVDF separately.

The extra PANI layering in patches over the existing PANI coating is responsible for causing uneven, coarse, and rough surface topography and membrane morphology because of a gradual increase in resin quantity. Similarly, micrographs 10(f) to (i) indicate that the membranes are based on PVDF blended with cation exchange resin in the ratio of 90:10, 80:20, 70:30, and 60:40, respectively. Moving from image 10.[f] to 10.[i], the careful inspection reveals that the PANI-coating is uneven, scaly, and rough with slight agglomeration due to a gradual increase and decrease of resin and PVDF quantity in the membrane. The tiny, microscopic

spheres of PVDF and styrene are interconnected to each other, developing channels and offering heterogeneous structures inside the IEM, showing a rough surface, promoting better PANI adsorption. The uneven distribution of the hydrophobic and hydrophilic domains throughout the membrane matrix leads to heterogeneous morphological character, which facilitates the development of continuous and expanded ion-conducting and shifting channels for enhanced ionic movement. Anions surround the backbone of the PVDF molecule, and these anions are distributed along every side of the chain. When the interconnected-based separation is decreased, the hydrophilicity increases due to the motion and conduction of ions [112]. The bulky PVDF hydrophobic segments within the side chains of the hydrophilic segment play a vital role in developing a hydrophobic domain. SEM images identify two types of morphological and topographical appearance of the membrane structure., The one type is light in color and spherical, exhibiting a crystalline structure due to the PVDF, while the darker part is because of an amorphous phase corresponding to hydrophilic quaternized-VBC. The presence of two different structures within the membrane validates the heterogeneity in the membrane. The hydrophobic and hydrophilic micro-phase partition enhances the ion-conducting properties of the membrane. The shape, pore size, symmetry, and distribution become uneven and haphazard, leading to a rough, coarse, and somewhat uneven membrane surface [97]. This phenomenon can be explained by considering the strong polar nature of the sulphonic group in the mecolite PC0031D resin. A robust interaction has been noticed between the quinoid (-N=) or the benzenoid (N-H) part of the PANI with the sulphonic acid in cation exchange resin, and it may have resulted in a relatively thick and coarse coating of PANI partly covering the membrane surface. The extra-PANI layering via in situ polymerization in patches over the existing PANI-coating and gradually enhancing resin quantity from 10%, 20%,30%, and 40% has caused uneven, rough, and coarse surface morphology [113].

4.8. Electrodialysis:

Table 3 shows the electrodialysis results regarding the separation of glycine by applying the plain, and PANI-coating 15%PVDFmembrane and these membranes have separated 4% and 9.8% glycine respectively but when mecolite (PA101/PC0031D) was incorporated in the matrix of membranes than such membranes exhibited entirely different results in terms of their separation efficiencies. The PANI-coated IEMs containing 90% polymer and 10% resin have separated 10% of glycine, and when the quantity of resin is enhanced from 10% to 20%, and similarly, the polymer ratio is reduced from 90% to 80%, the glycine separation is enhanced from 10% to 24%. The enhanced resin quantity has enhanced the exchangeable chloride ions**.** These chloride ions have exchanged more glycinate ions, increasing the efficiency of AEM in terms of glycine separation. This trend goes on to improve the membrane efficiency with the increase in resin quantity. The consumption of energy varies from 1.4 to 0.7 kWh/kg during the process of electrodialysis whereas the variation in current efficiency (η) from 59% to 81% was also observed with an increasing trend of PANI-coating exhibiting enhanced membrane performance in terms of glycine separation due to an increase in resin quantity from 10% to 40% which is indirectly promoting the exchangeable chloride ions. IEMs are based on fixed charge moieties, and they only allow counterions to pass under the influence of the driving force, whereas the water molecules and the co-ions are rejected while obeying transport theory [114, 115]. Electrodialysis more conveniently separates the ionic substances through the IEM under the influence of an electric field, which functions as a driving force. The transport of ions is linked with the properties of ions, such as the kind of polymer matrix, crosslinking degree, and the ionic charge concentration, which is fixed on the ion [73]. The IEMs are used in electrolytic cells, where they permit the selective transportation of cations and anions as required [116]. Electrodialysis of a 1% glycine solution was conducted by using a PANI-coated,100µm µm-thick AEM, which acted as a test membrane.

The values in Table 3 indicate that there is a gradual increase in driving force, which indirectly indicates the enhanced performance of AEM in terms of separating glycinate ions in the form of concentrated glycine solution in the product chamber. The glycine separation results are summarized in Table 3. The glycine concentration taken from the feed and product chambers was ascertained by titrating it against 0.05 M HCl using phenolphthalein as an indicator [68] The results of the titration were confirmed by HPLC.MSMS.

4.9. HPLC.MSMS:

The separation of glycine was carried out as glycinate ion from a 1% glycine feed and product solutions by its electrodialysis using AEM at a constant 31.4V in 30 min. As the electrodialysis advances, the separation of glycine in the form of glycinate ion increases, which is evident from the increasing and decreasing volume of glycine in the product and feed chambers with the rise in temperature and vigorous bubbling in both chambers. The peak of glycine was identified at its retention time of 13.57 min, which is taken from the chromatograms produced by HPLC.MSMS in case of glycine feed and product solutions separately. Mass hunter software of MSMS was used to generate a quantitation report, and with its help 4-point calibration curve with linearity, R^2 = 0.996, was drawn. The membrane efficiency gradually enhanced in terms of glycine separation as the quantity of resin increased. The results verify the AEM efficiency, which has already been verified by the titration method.

5. Conclusion:

The composite anion and cation exchange membranes were synthesized by dispersing 10%, 20%, 30%, and 40% anion (mecolite PA101) and cation (mecolite PC0031D) exchange resin separately in a 15% PVDF matrix used as the base polymer. Similarly, the pristine membrane was synthesized using pure PVDF. Subsequently**,** each membrane was modified with PANI coating except the pristine membrane. SEM images of membranes showed that the pore size, symmetry, smoothness, and texture of the PANI film depend upon the quantity, distribution, size, and shape of resin particles incorporated during the synthesis process in the PVDF matrix. The ultrafine texture and smooth surface of the membranes depend upon the thickness and structure of the PANI film, which is controlled by the nature of the oligomers and the duration of in situ polymerization. The enhanced duration and relatively large size promote PANI film's dense and rough texture, while the fine size may lead to a smooth and groove-free surface. The experimental data regarding electrical conductivity elucidate that while enhancing the PANI-coating and resin quantity, the electrical conductivity of the IEM increases, and the IEM becomes more conductive, which helps in increasing its efficiency. The interaction between PVDF, anion, and cation exchange resin in the membrane was established by FTIR, in addition to surface coating with PANI by hydrogen bonding among them. The gradual increase in resin quantity favors more exchangeable chloride ions, and these ions can separate more glycinate ions; as such, it enhances the efficiency of AEM from 10% to 43% in terms of glycine separation. The results and data of experiments indicated that the capability of an AEM can be enhanced to separate the organic acids if the quantity of resin and PANI-coating is enhanced while using direct current as a potential source. Necessary measures may be taken to separate glycine and other organic acids from fermentation broths, including electrodysis, where there is a chance of their wastage during certain procedures due to discrepancies and flaws in the operational system. Separating glycine and other organic acids from waste, broths, and the places where they are deteriorating openly will save revenue in the form of precious products and also provide a better solution to the industries in terms of instant availability of raw material to prepare food supplements, energy drinks, beverages, and tonics.

6. Conflıct of ınterest:

The authors declare that they have no conflict of interest.

References:

[1] S. Al Aani, T. N. Mustafa, and N. J. J. o. W. P. E. Hilal, "Ultrafiltration membranes for wastewater and water process engineering: A comprehensive statistical review over the past decade," vol. 35, pp. 101241, 2020.

[2] B. Saini, M. K. Sinha, A. J. P. S. Dey, and E. Protection, "Functionalized polymeric smart membrane for remediation of emerging environmental contaminants from industrial sources: Synthesis, characterization and potential applications," vol. 161, pp. 684-702, 2022.

[3] G.-d. Kang, and Y.-m. J. J. o. m. s. Cao, "Application and modification of poly (vinylidene fluoride)(PVDF) membranes–a review," vol. 463, pp. 145-165, 2014.

[4] T. Otitoju, A. Ahmad, and B. J. J. o. W. P. E. Ooi, "Polyvinylidene fluoride (PVDF) membrane for oil rejection from oily wastewater: A performance review," vol. 14, pp. 41-59, 2016.

[5] S. Ebnesajjad, *Fluoroplastics, volume 2: Melt processible fluoropolymers-the definitive user's guide and data book*: William Andrew, 2015.

[6] B. J. C. r. Ameduri, "From vinylidene fluoride (VDF) to the applications of VDF-containing polymers and copolymers: recent developments and future trends," vol. 109, no. 12, pp. 6632-6686, 2009.

[7] P. Martins, A. Lopes, and S. J. P. i. p. s. Lanceros-Mendez, "Electroactive phases of poly (vinylidene fluoride): Determination, processing and applications," vol. 39, no. 4, pp. 683-706, 2014.

[8] I. G. J. D. Wenten, "Reverse osmosis applications: Prospect and challenges," vol. 391, pp. 112-125, 2016.

[9] M. Reig, H. Farrokhzad, B. Van der Bruggen, O. Gibert, and J. L. J. D. Cortina, "Synthesis of a monovalent selective cation exchange membrane to concentrate reverse osmosis brines by electrodialysis," vol. 375, pp. 1-9, 2015.

[10] C. Boo, J. Lee, M. J. E. s. Elimelech, and technology, "Omniphobic polyvinylidene fluoride (PVDF) membrane for desalination of shale gas produced water by membrane distillation," vol. 50, no. 22, pp. 12275-12282, 2016.

[11] H. J. D. Strathmann, "Electrodialysis, a mature technology with a multitude of new applications," vol. 264, no. 3, pp. 268-288, 2010.

[12] G. J. D. Pourcelly, "Conductivity and selectivity of ion exchange membranes: structure-correlations," vol. 147, no. 1-3, pp. 359-361, 2002.

[13] S. Yonezawa, K. Kanamura, and Z. i. J. J. o. T. E. S. Takehara, "Discharge and charge characteristics of polyaniline prepared by electropolymerization of aniline in nonaqueous solvent," vol. 140, no. 3, pp. 629, 1993.

[14] J. Labanda, J. Sabaté, and J. Llorens, "Experimental and modeling study of the adsorption of single and binary dye solutions with an ion-exchange membrane adsorber," *Chemical Engineering Journal,* vol. 166, no. 2, pp. 536-543, 2011/01/15/, 2011.

[15] S. Jiang, H. Sun, H. Wang, B. P. Ladewig, and Z. J. C. Yao, "A comprehensive review on the synthesis and applications of ion exchange membranes," vol. 282, pp. 130817, 2021.

[16] R. Nagarale, G. Gohil, V. K. Shahi, G. Trivedi, R. J. J. o. C. Rangarajan, and I. Science, "Preparation and electrochemical characterization of cation-and anion-exchange/polyaniline composite membranes," vol. 277, no. 1, pp. 162-171, 2004.

[17] M. Mulder, *Basic principles of membrane technology*: Springer science & business media, 1996.

[18] H. Farrokhzad, M. Moghbeli, T. Van Gerven, B. J. R. Van der Bruggen, and F. Polymers, "Surface modification of composite ion exchange membranes by polyaniline," vol. 86, pp. 161-167, 2015.

[19] B. J. Ryan, and C. J. B. b. Ó'Fágáin, "Arginine-to-lysine substitutions influence recombinant horseradish peroxidase stability and immobilisation effectiveness," vol. 7, pp. 1-9, 2007.

[20] K. J. I. J. o. C. Matyjaszewski, "Atom transfer radical polymerization: from mechanisms to applications," vol. 52, no. 3-4, pp. 206-220, 2012.

[21] M. Aghmasheh, M. A. Rezvani, V. Jafarian, and Z. J. I. C. Aghasadeghi, "High Oxidation Desulfurization of Fuels Catalyzed by Vanadium-Substituted Phosphomolybdate@ Polyaniline@ Chitosan as an Inorganic–Organic Hybrid Nanocatalyst," 2023.

[22] D. Chinn, and J. J. T. S. F. Janata, "Spin-cast thin films of polyaniline," vol. 252, no. 2, pp. 145-151, 1994.

[23] H. Zeghioud, S. Lamouri, Z. Safidine, and M. J. J. o. t. S. C. S. Belbachir, "Chemical synthesis and characterization of highly soluble conducting polyaniline in mixtures of common solvents," vol. 80, no. 7, pp. 917–931-917–931, 2015.

[24] G. R. Guillen, Y. Pan, M. Li, E. M. J. I. Hoek, and E. C. Research, "Preparation and characterization of membranes formed by nonsolvent induced phase separation: a review," vol. 50, no. 7, pp. 3798-3817, 2011.

[25] J. Stejskal, I. Sapurina, and M. J. P. i. P. S. Trchová, "Polyaniline nanostructures and the role of aniline oligomers in their formation," vol. 35, no. 12, pp. 1420-1481, 2010.

[26] T. J. J. o. M. S. Sata, "Studies on anion exchange membranes having permselectivity for specific anions in electrodialysis—effect of hydrophilicity of anion exchange membranes on permselectivity of anions," vol. 167, no. 1, pp. 1-31, 2000.

[27] R. W. Baker, *Membrane technology and applications*: John Wiley & Sons, 2023.

[28] A. Montes-Rojas, J. Rentería, N. Chávez, J. Ávila-Rodríguez, and B. Y. J. R. a. Soto, “Influence of anion hydration status on selective properties of a commercial anion exchange membrane electrochemically impregnated with polyaniline deposits,” vol. 7, no. 41, pp. 25208-25219, 2017.

[29] P. C. Wang, Z. Huang, and A. G. MacDiarmid, “Critical dependency of the conductivity of polypyrrole and polyaniline films on the hydrophobicity/hydrophilicity of the substrate surface,” *Synthetic Metals,* vol. 101, no. 1, pp. 852-853, 1999/05/01/, 1999.

[30] I. Sapurina, A. Riede, and J. J. S. M. Stejskal, “In-situ polymerized polyaniline films: 3. Film formation,” vol. 123, no. 3, pp. 503-507, 2001.

[31] A. G. MacDiarmid, “Polyaniline and polypyrrole: Where are we headed?,” *Synthetic Metals,* vol. 84, no. 1, pp. 27-34, 1997/01/01/, 1997.

[32] S. Zhu, M. Shi, S. Zhao, Z. Wang, J. Wang, and S. J. R. a. Wang, “Preparation and characterization of a polyethersulfone/polyaniline nanocomposite membrane for ultrafiltration and as a substrate for a gas separation membrane,” vol. 5, no. 34, pp. 27211-27223, 2015.

[33] P. He, S. Zhao, C. Mao, Y. Wang, G. Ma, Z. Wang, and J. J. C. E. J. Wang, “In-situ growth of double-layered polyaniline composite membrane for organic solvent nanofiltration,” vol. 420, pp. 129338, 2021.

[34] M. E. Butler, A. J. J. S. Brant, and P. Technology, “Emulsion separation and fouling of electrospun polyacrylonitrile membranes for produced water applications,” vol. 306, pp. 122623, 2023.

[35] Khurram, A. A. Qaiser, A. Ghaffar, A. Munawar, N. S. Ali, T. Hussain, and R. J. R. J. o. E. Saleem, “Development of polyaniline based anion exchange membrane for the separation of lactic acid via electrodialysis,” vol. 56, pp. 587-595, 2020.

[36] C. Xu, W. Wei, and Y. J. M. L. He, “Enhanced hydrogen separation performance of Linde Type-A zeolite molecular sieving membrane by cesium ion exchange,” vol. 324, pp. 132680, 2022.

[37] S. Hosseini, P. Koranian, A. Gholami, S. Madaeni, A. Moghadassi, P. Sakinejad, and A. J. D. Khodabakhshi, “Fabrication of mixed matrix heterogeneous ion exchange membrane by multiwalled carbon nanotubes: Electrochemical characterization and transport properties of mono and bivalent cations,” vol. 329, pp. 62-67, 2013.

[38] C. K. Mathews, K. Van Holde, and K. J. M. P. Ahern, CA, “Biochemistry Benjamin Cummings,” pp. 670-703, 1990.

[39] P. Mandal, R. Mondal, P. Goel, E. Bhuvanesh, U. Chatterjee, S. J. S. Chattopadhyay, and P. Technology, “Selective recovery of carboxylic acid through PVDF blended anion exchange membranes using electrodialysis,” vol. 292, pp. 121069, 2022.

[40] D.-E. Akretche, and H. J. T. Kerdjoudj, “Donnan dialysis of copper, gold and silver cyanides with various anion exchange membranes,” vol. 51, no. 2, pp. 281-289, 2000.

[41] N. ÜNLÜ, H. KARA, and M. J. T. J. o. C. ERSÖZ, “Glycine transport through a charged polysulfone cation exchange membrane,” vol. 26, no. 2, pp. 211-220, 2002.

[42] C. Huang, T. Xu, Y. Zhang, Y. Xue, and G. J. J. o. m. s. Chen, “Application of electrodialysis to the production of organic acids: State-of-the-art and recent developments,” vol. 288, no. 1-2, pp. 1-12, 2007.

[43] A. Chandra, E. Bhuvanesh, S. J. C. E. R. Chattopadhyay, and Design, “A critical analysis on ion transport of organic acid mixture through an anion-exchange membrane during electrodialysis,” vol. 178, pp. 13-24, 2022.

[44] V. Hábová, K. Melzoch, M. Rychtera, and B. J. D. Sekavová, “Electrodialysis as a useful technique for lactic acid separation from a model solution and a fermentation broth,” vol. 162, pp. 361-372, 2004.

[45] H. Morker, B. Saini, and A. J. M. T. P. Dey, “Role of membrane technology in food industry effluent treatment,” vol. 77, pp. 314-321, 2023.

[46] M. Haponska, A. Trojanowska, A. Nogalska, R. Jastrzab, T. Gumi, and B. J. P. Tylkowski, “PVDF membrane morphology—Influence of polymer molecular weight and preparation temperature,” vol. 9, no. 12, pp. 718, 2017.

[47] X. Dong, D. Lu, T. A. Harris, and I. C. J. M. Escobar, “Polymers and solvents used in membrane fabrication: a review focusing on sustainable membrane development,” vol. 11, no. 5, pp. 309, 2021.

[48] J. E. Marshall, A. Zhenova, S. Roberts, T. Petchey, P. Zhu, C. E. Dancer, C. R. McElroy, E. Kendrick, and V. J. P. Goodship, “On the solubility and stability of polyvinylidene fluoride,” vol. 13, no. 9, pp. 1354, 2021.

[49] H. Peng, V. Shah, and K. J. J. o. M. S. Li, “Morphology and performance of polyvinylidene fluoride (PVDF) membranes prepared by the CCD method: Thermodynamic considerations,” vol. 641, pp. 119857, 2022.

[50] Y. Deng, G. Zhang, R. Bai, S. Shen, X. Zhou, and I. J. J. o. M. S. Wyman, “Fabrication of superhydrophilic and underwater superoleophobic membranes via an in situ crosslinking blend strategy for highly efficient oil/water emulsion separation,” vol. 569, pp. 60-70, 2019.

[51] I. Y. Abdullah, M. Yahaya, M. H. H. Jumali, and H. M. Shanshool, "Effect of annealing process on the phase formation in poly (vinylidene fluoride) thin films." pp. 147-151.

[52] M. S. Malik, A. A. Qaiser, and M. A. J. R. a. Arif, “Structural and electrochemical studies of heterogeneous ion exchange membranes based on polyaniline-coated cation exchange resin particles,” vol. 6, no. 116, pp. 115046-115054, 2016.

[53] A. Ghaffar, S. Zulfiqar, M. Khan, M. Latif, and E. W. J. R. a. Cochran, “Synthesis of polyaniline-coated composite anion exchange membranes based on polyacrylonitrile for the separation of tartaric acid via electrodialysis,” vol. 14, no. 40, pp. 29648-29657, 2024.

[54] L. F. Malmonge, G. d. A. Lopes, S. d. C. Langiano, J. A. Malmonge, J. M. Cordeiro, and L. H. C. J. E. P. J. Mattoso, “A new route to obtain PVDF/PANI conducting blends,” vol. 42, no. 11, pp. 3108-3113, 2006.

[55] E. J. D. Stránská, and W. Treatment, “Relationships between transport and physical–mechanical properties of ion exchange membranes,” vol. 56, no. 12, pp. 3220-3227, 2015.

[56] P. Bulejko, E. J. M. C. Stránská, and Physics, “The effect of initial moisture content of cation-exchange resin on the preparation and properties of heterogeneous cation-exchange membranes,” vol. 205, pp. 470-479, 2018.

[57] R. Kingsbury, S. Zhu, S. Flotron, O. J. A. a. m. Coronell, and interfaces, “Microstructure determines water and salt permeation in commercial ion-exchange membranes,” vol. 10, no. 46, pp. 39745-39756, 2018.

[58] A. Hassanvand, K. Wei, S. Talebi, G. Q. Chen, and S. E. J. M. Kentish, “The role of ion exchange membranes in membrane capacitive deionisation,” vol. 7, no. 3, pp. 54, 2017.

[59] H. A. Ezzeldin, A. Apblett, and G. L. J. I. J. o. P. S. Foutch, “Synthesis and properties of anion exchangers derived from chloromethyl styrene codivinylbenzene and their use in water treatment,” vol. 2010, 2010.

[60] S. Sharma, M. Dinda, C. R. Sharma, and P. K. J. J. o. m. s. Ghosh, “A safer route for preparation of anion exchange membrane from inter-polymer film and performance evaluation in electrodialytic application,” vol. 459, pp. 122-131, 2014.

[61] L. Dominguez, J. Economy, K. Benak, and C. L. J. P. f. A. T. Mangun, “Anion exchange fibers for arsenate removal derived from a vinylbenzyl chloride precursor,” vol. 14, no. 9, pp. 632-637, 2003.

[62] S. Melnikov, O. Mugtamov, V. J. S. Zabolotsky, and P. Technology, “Study of electrodialysis concentration process of inorganic acids and salts for the two-stage conversion of salts into acids utilizing bipolar electrodialysis,” vol. 235, pp. 116198, 2020.

[63] M. I. Khan, R. Luque, S. Akhtar, A. Shaheen, A. Mehmood, S. Idress, S. A. Buzdar, and A. Ur Rehman, “Design of Anion Exchange Membranes and Electrodialysis Studies for Water Desalination,” vol. 9, no. 5, pp. 365, 2016.

[64] Z. A. ALOthman, M. M. Alam, M. Naushad, and R. J. I. J. E. S. Bushra, “Electrical conductivity and thermal stability studies on polyaniline Sn (IV) tungstomolybdate nanocomposite cation exchange material: application as Pb (II) ion-selective membrane electrode,” vol. 10, no. 3, pp. 2663-2684, 2015.

[65] F. M. SMITS, “Measurement of Sheet Resistivities with Four-Point Probe,” *THE BELL SYSTEM TECHNICAL JOURNAL*, MAY, 1958.

[66] F. J. B. S. T. J. Smits, “Measurement of sheet resistivities with the four-point probe,” vol. 37, no. 3, pp. 711-718, 1958.

[67] A. A. Qaiser, R. Saleem, N. S. Ali, S. Nazir, T. Hussain, and A. J. T. J. o. C. Ghaffar, "Development of thermoplastic polyurethane/polyaniline-doped membranes forthe separation of glycine through electrodialysis," vol. 44, no. 1, pp. 224-236, 2020.

[68] R.-q. Guo, B.-b. Wang, Y.-x. Jia, M. J. S. Wang, and P. Technology, "Development of acid block anion exchange membrane by structure design and its possible application in waste acid recovery," vol. 186, pp. 188-196, 2017.

[69] H. W. J. J. o. t. A. C. S. Doughty, "Mohr's method for the determination of silver and halogens in other than neutral solutions," vol. 46, no. 12, pp. 2707-2709, 1924.

[70] W. Liang, Y. Chenyang, Z. Bin, W. Xiaona, Y. Zijun, Z. Lixiang, Z. Hongwei, and L. J. J. o. m. s. Nanwen, "Hydrophobic polyacrylonitrile membrane preparation and its use in membrane contactor for CO2 absorption," vol. 569, pp. 157-165, 2019.

[71] S. Huysman, F. Vanryckeghem, E. De Paepe, F. Smedes, S. A. Haughey, C. T. Elliott, K. Demeestere, L. J. E. s. Vanhaecke, and technology, "Hydrophilic divinylbenzene for equilibrium sorption of emerging organic contaminants in aquatic matrices," vol. 53, no. 18, pp. 10803-10812, 2019.

[72] M. Akter, and J.-S. J. M. Park, "Fouling and Mitigation Behavior of Foulants on Ion Exchange Membranes with Surface Property in Reverse Electrodialysis," vol. 13, no. 1, pp. 106, 2023.

[73] F. Amado, L. Rodrigues Jr, M. Rodrigues, A. Bernardes, J. Ferreira, and C. J. D. Ferreira, "Development of polyurethane/polyaniline membranes for zinc recovery through electrodialysis," vol. 186, no. 1-3, pp. 199-206, 2005.

[74] J. Weiss, M. Voigt, C. Kunze, J. H. Sánchez, W. Possart, G. J. I. J. o. A. Grundmeier, and Adhesives, "Ageing mechanisms of polyurethane adhesive/steel interfaces," vol. 70, pp. 167-175, 2016.

[75] M. Ahmad, A. A. Qaiser, N. U. Huda, and A. J. R. a. Saeed, "Heterogeneous ion exchange membranes based on thermoplastic polyurethane (TPU): Effect of PSS/DVB resin on morphology and electrodialysis," vol. 10, no. 6, pp. 3029-3039, 2020.

[76] F.-S. Yen, L.-L. Lin, and J.-L. J. M. Hong, "Hydrogen-bond interactions between urethane− urethane and urethane− ester linkages in a liquid crystalline poly (ester− urethane)," vol. 32, no. 9, pp. 3068-3079, 1999.

[77] P. Hillis, *Membrane technology in water and wastewater treatment*: Royal Society of Chemistry, 2000.

[78] M. Mulder, *Basic principles of membrane technology*: Springer science & business media, 2012.

[79] O. Petrov, N. Iwaszczuk, I. Bejanidze, T. Kharebava, V. Pohrebennyk, N. Didmanidze, and N. J. M. Nakashidze, "Study of the Electrical Conductivity of Ion-Exchange Resins and Membranes in Equilibrium Solutions of Inorganic Electrolytes," vol. 12, no. 2, pp. 243, 2022.

[80] J. C. Díaz, and J. J. J. o. M. S. Kamcev, "Ionic conductivity of ion-exchange membranes: Measurement techniques and salt concentration dependence," vol. 618, pp. 118718, 2021.

[81] N. Carboni, L. Mazzapioda, A. Caprì, I. Gatto, A. Carbone, V. Baglio, and M. A. J. E. A. Navarra, "Composite anion exchange membranes based on graphene oxide for water electrolyzer applications," vol. 486, pp. 144090, 2024.

[82] R.-Y. Chang, R. Li, W. Wang, W.-H. Geng, N. Li, L.-C. Jing, Z.-X. Yang, J. Li, and H.-Z. J. J. o. M. S. Geng, "Electrical responsiveness of carboxylate multi-walled carbon nanotube cross-linked composite anti-fouling membranes to organic pollutants," vol. 693, pp. 122360, 2024.

[83] J. Hao, L. Wang, X. Wang, J. Wang, M. He, X. Zhang, J. Wang, L. Nie, J. J. E. S. W. R. Li, and Technology, "Preparation, modification and antifouling properties of polyaniline conductive membranes for water treatment: a comprehensive review," 2023.

[84] M. Beygisangchin, S. Abdul Rashid, S. Shafie, A. R. Sadrolhosseini, and H. N. J. P. Lim, "Preparations, properties, and applications of polyaniline and polyaniline thin films—A review," vol. 13, no. 12, pp. 2003, 2021.

[85] S. Barrau, A. Ferri, A. Da Costa, J. Defebvin, S. Leroy, R. Desfeux, J.-M. J. A. a. m. Lefebvre, and

interfaces, “Nanoscale investigations of α-and γ-crystal phases in PVDF-based nanocomposites,” vol. 10, no. 15, pp. 13092-13099, 2018.

[86] P. Kaspar, D. Sobola, K. Částková, A. Knápek, D. Burda, F. Orudzhev, R. Dallaev, P. Tofel, T. Trčka, and L. J. P. Grmela, “Characterization of polyvinylidene fluoride (PVDF) electrospun fibers doped by carbon flakes,” vol. 12, no. 12, pp. 2766, 2020.

[87] S. Lanceros-Mendez, J. Mano, A. Costa, and V. H. J. J. o. M. S. Schmidt, Part B, “FTIR and DSC studies of mechanically deformed β-PVDF films,” vol. 40, no. 3-4, pp. 517-527, 2001.

[88] A. Salimi, and A. A. J. P. T. Yousefi, “Analysis method: FTIR studies of β-phase crystal formation in stretched PVDF films,” vol. 22, no. 6, pp. 699-704, 2003.

[89] A. A. Issa, M. Al-Maadeed, A. S. Luyt, M. Mrlik, and M. K. J. J. o. A. P. S. Hassan, “Investigation of the physico-mechanical properties of electrospun PVDF/cellulose (nano) fibers,” vol. 133, no. 26, 2016.

[90] C. Constantino, A. Job, R. Simoes, J. Giacometti, V. Zucolotto, O. Oliveira, G. Gozzi, and D. Chinaglia, "The Investigation of/spl alpha//spl rArr//spl beta/phase transition in poly (vinylidene fluoride)(PVDF)." pp. 178-181.

[91] H. H. Singh, S. Singh, and N. J. P. f. A. T. Khare, “Enhanced β-phase in PVDF polymer nanocomposite and its application for nanogenerator,” vol. 29, no. 1, pp. 143-150, 2018.

[92] F. Orudzhev, S. Ramazanov, D. Sobola, P. Kaspar, T. Trčka, K. Částková, J. Kastyl, I. Zvereva, C. Wang, and D. J. N. E. Selimov, “Ultrasound and water flow driven piezophototronic effect in self-polarized flexible α-Fe2O3 containing PVDF nanofibers film for enhanced catalytic oxidation,” vol. 90, pp. 106586, 2021.

[93] E. Kabir, M. Khatun, L. Nasrin, M. J. Raihan, and M. J. J. o. P. D. A. P. Rahman, “Pure β-phase formation in polyvinylidene fluoride (PVDF)-carbon nanotube composites,” vol. 50, no. 16, pp. 163002, 2017.

[94] X. Cai, T. Lei, D. Sun, and L. J. R. a. Lin, “A critical analysis of the α, β and γ phases in poly (vinylidene fluoride) using FTIR,” vol. 7, no. 25, pp. 15382-15389, 2017.

[95] Y. Nie, F. Chen, W. Zhao, H. Zhang, S. Wang, X. Sun, S. J. I. Yan, and E. C. Research, “Validity of–CF2 Band Shift in Poly (vinylidene fluoride) as an Indicator for the Ion–Dipole Interaction,” vol. 63, no. 13, pp. 5970-5976, 2024.

[96] R. Gregorio Jr, and N. C. P. J. J. o. P. D. A. P. de Souza Nociti, “Effect of PMMA addition on the solution crystallization of the alpha and beta phases of poly (vinylidene fluoride)(PVDF),” vol. 28, no. 2, pp. 432, 1995.

[97] P. P. Sharma, V. Yadav, A. Rajput, and V. J. D. Kulshrestha, “PVDF-g-poly (styrene-co-vinylbenzyl chloride) based anion exchange membrane: High salt removal efficiency and stability,” vol. 444, pp. 35-43, 2018.

[98] Y. Cao, P. Smith, and A. J. S. M. Heeger, “Spectroscopic studies of polyaniline in solution and in spin-cast films,” vol. 32, no. 3, pp. 263-281, 1989.

[99] N. V. Bhat, D. T. Seshadri, and R. S. J. S. m. Phadke, “Simultaneous polymerization and crystallization of aniline,” vol. 130, no. 2, pp. 185-192, 2002.

[100] M. Şahin, H. Görçay, E. Kır, Y. J. R. Şahin, and F. Polymers, “Removal of calcium and magnesium using polyaniline and derivatives modified PVDF cation-exchange membranes by Donnan dialysis,” vol. 69, no. 9, pp. 673-680, 2009.

[101] S. Begum, H. Ullah, I. Ahmed, Y. Zhan, A. Kausar, M. A. Aleem, S. J. C. S. Ahmad, and Technology, “Investigation of morphology, crystallinity, thermal stability, piezoelectricity and conductivity of PVDF nanocomposites reinforced with epoxy functionalized MWCNTs,” vol. 211, pp. 108841, 2021.

[102] A. LOVINGER, "Developments in crystalline polymers London," Applied Science Publishers Ltd., pag, 1982.

[103] S. Zulfiqar, M. Zulfiqar, M. Rizvi, A. Munir, I. J. P. D. McNeill, and Stability, “Study of the thermal degradation of polychlorotrifluoroethylene, poly (vinylidene fluoride) and copolymers of chlorotrifluoroethylene and vinylidene fluoride,” vol. 43, no. 3, pp. 423-430, 1994.

[104] J. A. Conklin, S.-C. Huang, S.-M. Huang, T. Wen, and R. B. J. M. Kaner, “Thermal Properties of Polyaniline and Poly (aniline-co-o-

ethylaniline)," vol. 28, no. 19, pp. 6522-6527, 1995.

[105] S. Sinha, S. Bhadra, and D. J. J. o. A. P. S. Khastgir, "Effect of dopant type on the properties of polyaniline," vol. 112, no. 5, pp. 3135-3140, 2009.

[106] L. Malmonge, and L. J. P. Mattoso, "Thermal analysis of conductive blends of PVDF and poly (o-methoxyaniline)," vol. 41, no. 23, pp. 8387-8391, 2000.

[107] M. M. Ostwal, J. Pellegrino, I. Norris, T. T. Tsotsis, M. Sahimi, B. R. J. I. Mattes, and e. c. research, "Water sorption of acid-doped polyaniline solid fibers: equilibrium and kinetic response," vol. 44, no. 20, pp. 7860-7867, 2005.

[108] M. E. Brown, *Introduction to thermal analysis: techniques and applications*: Springer, 2001.

[109] X. Zuo, W. Shi, S. Yu, J. J. W. S. He, and Technology, "Fundamental characteristics study of anion-exchange PVDF–SiO2 membranes," vol. 66, no. 11, pp. 2343-2348, 2012.

[110] Z. Jia, F. Li, X. Zhang, and X. J. C. E. J. Zhao, "Effects of cation exchange membrane properties on the separation of salt from high-salt organic wastewater by electrodialysis," vol. 475, pp. 146287, 2023.

[111] H. J. C. E. Isawi, and P.-P. Intensification, "Synthesis of graphene oxide-silver (GO-Ag) nanocomposite TFC RO membrane to enhance morphology and separation performances for groundwater desalination,(case study Marsa Alam area-Red Sea)," vol. 187, pp. 109343, 2023.

[112] I. Stenina, D. Golubenko, V. Nikonenko, and A. Yaroslavtsev, "Selectivity of Transport Processes in Ion-Exchange Membranes: Relationship with the Structure and Methods for Its Improvement," vol. 21, no. 15, pp. 5517, 2020.

[113] Y. Zhang, L. Zou, B. P. Ladewig, and D. J. D. Mulcahy, "Synthesis and characterisation of superhydrophilic conductive heterogeneous PANI/PVDF anion-exchange membranes," vol. 362, pp. 59-67, 2015.

[114] M. Tedesco, H. Hamelers, and P. J. J. o. M. S. Biesheuvel, "Nernst-Planck transport theory for (reverse) electrodialysis: II. Effect of water transport through ion-exchange membranes," vol. 531, pp. 172-182, 2017.

[115] A. A. Sonin, and R. F. J. D. Probstein, "A hydrodynamic theory of desalination by electrodialysis," vol. 5, no. 3, pp. 293-329, 1968.

[116] H. Meng, L. Xiao, L. Li, C. J. D. Li, and W. Treatment, "Concentration of ionic liquids from aqueous ionic liquids solution using electrodialyzer," vol. 34, no. 1-3, pp. 326-329, 2011.